

NONLINEAR INTERFACE CRACK PROPAGATION IN CONCRETE GRAVITY DAMS UNDER SEISMIC LOADING

Marco Paggi, Giuseppe Ferro

Department of Structural and Geotechnical Engineering, Politecnico di Torino, C.so Duca degli Abruzzi 24, 10129 Torino, Italy

ABSTRACT

In this paper, the phenomenon of interface crack propagation in concrete gravity dams under seismic loading is addressed. This problem is particularly important from the engineering point of view. In fact, besides Mixed-Mode crack growth in concrete, dam failure is often the result of crack propagation along the rock-concrete interface at the dam foundation. To analyze such a problem, the generalized interface constitutive law recently proposed by the first author is used to properly model the phenomenon of crack closing and reopening at the interface. A damage variable is also introduced in the cohesive zone formulation in order to predict crack propagation under repeated loadings. Numerical examples will show the capabilities of the proposed approach applied to concrete gravity dams.

KEYWORDS

Interface crack propagation, nonlinear fracture mechanics, concrete dams, seismic loading

INTRODUCTION

Structural integrity assessment of concrete gravity dams has long been investigated (see, e.g., the recently established NW-IALAD research network). So far, most of the proposed numerical models based either on linear elastic [1-9] or nonlinear fracture mechanics [10, 11] concerned the simulation of Mixed-Mode crack propagation into concrete under hydraulic and weight loads. Experimental tests on scaled down models have also been performed in the past [12] to assess the reliability of linear elastic fracture mechanics (LEFM) predictions. On the other hand, seismic fracture analyses are quite scarce due to their high complexity [11,13,14]. Cracks encountered in dams require special modelling when subjected to crack closure, as it happens during repeated loadings [14]. When nonlinear fracture mechanics (NLFM) models are used, a nonlinear dynamic problem has to be solved [11], which is nowadays challenging due to the large differences in the characteristic time scales of the problem.

In the present paper, the problem of crack propagation at the interface between the concrete dam and the rock foundation is investigated. This source of damage is particularly important from the structural integrity point of view. In fact, besides Mixed-Mode crack growth in concrete, dam failure is often the result of crack propagation along the rock-concrete interface at the dam foundation. In this case, there is a lack of predictive models in the literature, especially for seismic analyses. To this aim, the generalized interface constitutive law proposed in [15] is used to properly model the phenomenon of crack closing and reopening at the interface. A damage variable is suitably introduced in the cohesive zone formulation in order to predict crack propagation under repeated loadings. A real case study is reported in the paper showing the capabilities of the proposed approach.

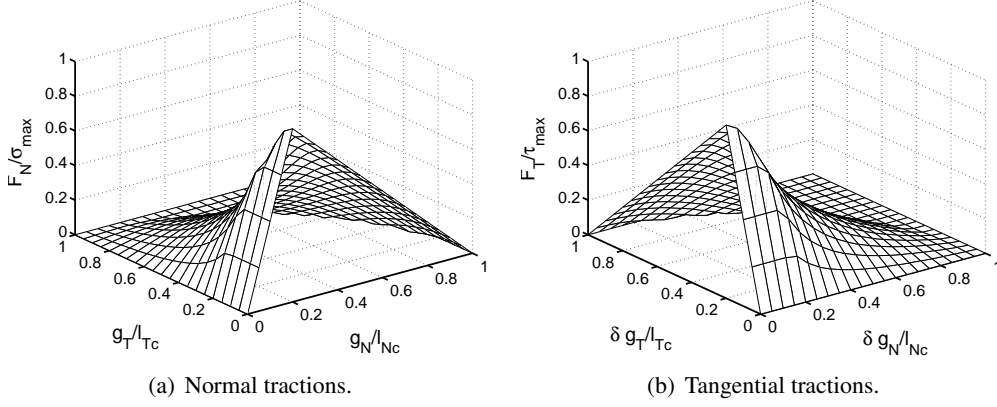


Figure 1: Normal and tangential tractions vs. normal and tangential separations for $\lambda_{\max} = 0.2$.

NUMERICAL MODEL

Cohesive zone model

Interface fracture between concrete and rock is herein modelled in the framework of NLFM, using the interface cohesive zone model proposed by Geubelle and Baylor [16]. This model, originally applied to composite materials, represents a natural extension of the classical bilinear cohesive zone models to Mixed-Mode interface crack problems, where Mode Mixity is usually an important issue that cannot be disregarded. Following this approach, a measure of interface opening and sliding, λ , is introduced:

$$\lambda = \sqrt{\left(\frac{g_N}{l_{Nc}}\right)^2 + \left(\frac{g_T}{l_{Tc}}\right)^2}, \quad (1)$$

where g_N and g_T denote, respectively, the normal and the tangential separations. Parameters l_{Nc} and l_{Tc} are the critical values for the normal and the tangential gap. They correspond to the separation for which cohesive forces transmitted through the interface vanish, i.e., complete debonding takes place. Normal and tangential cohesive tractions are given as functions of interface opening in the process zone:

$$F_N = \begin{cases} \frac{\sigma_{\max}}{\lambda_{\max}} \frac{g_N}{l_{Nc}} & 0 < \lambda \leq \lambda_{\max}, \\ \frac{\sigma_{\max}}{\lambda} \frac{1 - \lambda}{1 - \lambda_{\max}} \frac{g_N}{l_{Nc}} & \lambda_{\max} < \lambda < 1; \end{cases} \quad (2)$$

$$F_T = \begin{cases} \frac{\tau_{\max}}{\lambda_{\max}} \frac{l_{Nc}}{l_{Tc}} \frac{g_T}{l_{Tc}} & 0 < \lambda \leq \lambda_{\max}, \\ \frac{\tau_{\max}}{\lambda} \frac{1 - \lambda}{1 - \lambda_{\max}} \frac{l_{Nc}}{l_{Tc}} \frac{g_T}{l_{Tc}} & \lambda_{\max} < \lambda < 1. \end{cases} \quad (3)$$

The effect of coupling between normal and tangential displacements upon normal and tangential tractions is shown in Fig. 1 for $\lambda_{\max} = 0.2$. For either pure normal separation (Mode I), i.e. for $g_T = 0$, or for pure tangential separation (Mode II), i.e. for $g_N = 0$, the classical bilinear cohesive laws are obtained as limit cases. The parameter λ_{\max} has not any specific influence on the numerical results, provided that it is chosen sufficiently small as compared to the unity to obtain a very stiff behaviour of the ascending branch of the cohesive law.

Contact model

Cohesive models can be used for studying the debonding stage, until a complete interfacial separation occurs. However, due to repeated loadings, a proper modeling of crack closure is also required in order to fully characterize the mechanical behavior of interfaces. This is achieved using the generalized interface constitutive law proposed in [15]. When interface closure takes place, the unilateral contact constraints are imposed, i.e.: (i) penetration is not allowed, i.e. $g_N \geq 0$; (ii) a closed gap between the bodies leads to compressive contact tractions, i.e., if $g_N = 0$, then $F_N < 0$. When the gap is open, tractions are either equal to zero (debonded interface) or are computed according to the cohesive zone model outlined in the previous section.

Therefore, in analogy with the continuum, where it is required the expression of the total potential energy of the mechanical system to set up the finite element formulation, the contact problem corresponds to finding the minimum of a functional under boundary conditions expressed in terms of inequalities [17]. In addition to the typical displacement unknowns of the finite element method, the non-compenetrability conditions give rise to another set of unknowns, corresponding to the contact forces, F_N , acting at each finite element node along the interface. In this framework, the numerical techniques for the solution of such problems can be grouped into two main categories: those that satisfy the geometrical non-compenetrability condition exactly, and those that satisfy this condition only in an approximate way. In this study, we adopt the penalty method, which belongs to the second category. This technique presents the advantage that the number of equations related to the continuum discretization is not increased in the analysis. This permits to deal with a positively defined stiffness matrix with constant dimensions. According to this approach, for a given value of the normal gap, g_N , the corresponding normal force, F_N , is computed as the product of a penalty parameter, C , and the current value of the interpenetration. Clearly, the unilateral constraint condition is recovered only for values of the penalty parameter tending to infinity.

As far as the response of the joint in the tangential direction is concerned, two different situations have to be considered: in the former, no tangential relative displacement occurs in the contact zone subjected to a tangential force, F_T . This behaviour is called stick. The latter is represented by a relative tangential displacement, g_T , along the contact interface, which is the so-called slip. Stick is equivalent to the case where the relative tangential velocity is zero. Hence, the stick condition can be obtained as [19]:

$$\dot{g}_T = 0. \quad (4)$$

This condition is formulated in the current configuration and thus, in general, it imposes a nonlinear constraint equation on the motion along the contact interface. Sliding takes place when the tangential forces are above a certain limit, and the contacting surfaces move relative to each other. In our model, sliding is described by the Coulomb law:

$$F_T = -f |F_N| \frac{\dot{g}_T}{|\dot{g}_T|}, \quad \text{if } |F_T| > f |F_N|, \quad (5)$$

where the parameter f denotes the friction coefficient, which may range from 0.6 to 0.3. In the sequel we set $f = 0.3$ as a worst case situation for the interface.

Damage model for repeated loadings

In addition to the above traction-separation relations describing the behaviour of interfaces under tension/compression, a description of the damage evolution has to be provided in order to capture finite life effects in the case of repeated loading. To this aim, the initial cohesive strengths, σ_{\max} and τ_{\max} are replaced at each step by the actual cohesive strengths, σ_{\max}^t and τ_{\max}^t , which take into account the degradation of the cohesive law:

$$\sigma_{\max}^t = \sigma_{\max}(1 - D), \quad \tau_{\max}^t = \tau_{\max}(1 - D), \quad (6)$$

where D is the damage variable.

To compute the current state of damage, a description of the evolution of damage has to be provided. For cyclic loading, the damage evolution equation has to characterize the failure of the cohesive zone model due to cycling at subcritical loads. As a fundamental hypothesis, we assume that the increment of damage is related to the increment of deformation times a function of the stress level, similarly to the model proposed by Roe and Siegmund [18]:

$$\dot{D} = \left(\frac{\Delta g}{g_{\max}} \right)^\alpha \left(\frac{F}{\sigma_{\max}^t} - \frac{F_{th}}{\sigma_{\max}} \right)^\beta \quad 0 \leq \dot{D} \leq 1, \quad (7)$$

where $g = \sqrt{g_N^2 + g_T^2}$ is the resultant separation at a given time step. Hence, $\Delta g = g^{t+\Delta t} - g^t$ represents the increment of deformation from one time step to next. The variable g_{\max} denotes the maximum nondimensional cumulative separation length to get the failure of the cohesive zone under cyclic loading. Finally, $F = \sqrt{F_N^2 + F_T^2}$ is the resultant traction and F_{th} is a threshold value under which no damage occurs. The two exponents α and β are related to the severity of damage.

It is important to notice that the summation of the separation increments Δg in Eq. (7) is extended to positive increments only. In practice, this implies that reloading contributes to damage accumulation, whereas unloading does not. To complete the formulation, the current damage is computed as:

$$D = \int_0^t \dot{D} dt. \quad (8)$$

Finite element algorithms

In the finite element formulation, the contributions of the nodal normal and tangential contact and cohesive forces are added to the global virtual work equation [19]:

$$\delta W = Ah (F_N \delta g_N + F_T \delta g_T), \quad (9)$$

where the symbol A denotes an assembly operator for all the interface nodes and h is the size of the finite element. A main difficulty with the analysis, stemming from the contact constraints and the imperfect bonding, is that the extension of the contact and debonded zones are unknown *a priori*, and the corresponding boundary value problem must be solved with an iterative method. The Newton-Raphson solution procedures commonly used for solving nonlinear problems require the determination of the tangent stiffness matrix. Consistent linearization of the equation set (9) leads to:

$$\begin{aligned} \Delta \delta W = & h \left(\frac{\partial F_N}{\partial g_N} \Delta g_N + \frac{\partial F_N}{\partial g_T} \Delta g_T \right) \delta g_N + h \left(\frac{\partial F_T}{\partial g_N} \Delta g_N + h \frac{\partial F_T}{\partial g_T} \Delta g_T \right) \delta g_T \\ & + h F_N \Delta \delta g_N + h F_T \Delta \delta g_T \end{aligned} \quad (10)$$

where the symbol δ has been used for variations and the symbol Δ denotes linearizations. Linearizations and variations of the normal and the tangential gaps can be obtained as in [20], as well as the discretized version of these expressions for a direct implementation in the finite element formulation based on the node-to-segment contact strategy.

Regarding the problem of interface discretization, a major difficulty stems from the large size of the dam as compared to the process zone size. In fact, we have two distinct length scales: one is related to the dam size, the so-called structural or macroscopic size, and the other is a microscopic length scale related to the size of the process zone in front of the crack tip. To correctly capture the progress of crack propagation, the size of the smallest finite element should be comparable with the process zone size. To obtain an accurate solution without refining the mesh for the continuum, we adopt the *virtual node technique* originally proposed by Zavarise et al. [21] and then applied to interface mechanical problems in

[20]. The basic idea underling this method consists in changing the integration scheme usually adopted in node-to-segment contact elements. The cohesive/contact contribution to the stiffness matrix and the internal force vector are in fact integrated on the contact element through a n -point Gauss integration scheme instead of a simpler 2-point Newton-Cotes integration formula. In this way, an arbitrary number of Gauss points can be specified inside each contact element along the interface, regardless of the discretization used for the continuum. Moreover, due to the cyclopic size of the dam, which requires the use of concretes with large diameters of the aggregates, suitable values for the fracture energy and the material tensile strength have to be considered. This is performed here according to the Multi Fractal Scaling Law proposed by Carpinteri [22] and experimentally validated in [23, 24]. As a consequence of the large structural size of the system, the fracture energy to be used in the numerical simulations is higher than that obtained from laboratory specimens. The opposite trend takes place for the tensile strength.

Moreover, another difficulty regards the use of cohesive zone models in dynamics. This often leads to rate-dependent numerical results, although the description of the material behaviour does not explicitly include rate-dependent parameters (see [25] for a wide discussion on this topic). Numerical rate effects are due to the interplay between characteristic scales (length and time) of cohesive models and inertia. In particular, a very high loading rate seems to increase the peak stresses σ_{\max} and τ_{\max} and the fracture energy of the cohesive zone model with respect to a quasi-static analysis. This can be accounted for in the model by including a loading rate-dependency in the cohesive zone model, as proposed in [25]. However, this effect is not considered here for two reasons: there is a lack of experimental information about the dynamic behaviour of real rock-concrete interfaces and the use of the same cohesive parameters as for the quasi-static case is in favor of safety. In any case, two characteristic time scales should be considered:

$$t_1 = \frac{\rho c_L l_{nc}}{2\sigma_{\max}}, \quad t_2 = \frac{a_0}{c_L}, \quad (11)$$

where $c_L = \sqrt{E/\rho}$ is the dilatational wave speed of the material, computed as the square root of the ratio between the Young's modulus and the mass density, and a_0 is the free length of the interface in front to the crack tip. Therefore, t_1 is the intrinsic time of the cohesive zone model operating in dynamics and therefore it is proportional to the time requested by a dilatational wave to cross the process zone. The other time, t_2 , comes from the fact we are analyzing a structural problem with finite boundaries in dynamics. To deal with this two very different time scales, time integration is performed by using the Newmark formulae, explicit in the displacements and implicit in the velocities.

NUMERICAL APPLICATION

In this section, a numerical application of the proposed numerical model is presented for the analysis of separation at the cold interface between rock and concrete under the action of seismic loading. In order to analyze the effects of a real earthquake, we focus our attention on the Koyna dam geometry, for which the ground accelerations were recorded and are used as input for the dynamic problem (see Fig. 2 for the geometry and the undeformed mesh of the dam). The duration of the earthquake was nearly 9 s, with accelerations peaks up to 0.4 g (see the data in [11]). In addition to the dynamic excitation, the idrostatic pressure and the dead load are also considered in the simulation. Regarding the dynamic solution, a Rayleigh damping model is considered as in [14], with the damping matrix linearly expressed in terms of the mass and stiffness matrices. The Newmark parameters were also chosen as in [14] and we adopt a time step of 2.0 ms.

Regarding the parameters of the cohesive zone model, we set the interface fracture energy equal to 250 N/m and the peak strengths $\sigma_{\max} = \tau_{\max} = 3$ MPa (recent experimental results suggest that σ_{\max} and τ_{\max} have similar to each other [26]). As far as the damage model is concerned, we set $\beta = 0$ and we consider two cases, one with $\alpha = 1$ and another with $\alpha = 2$.

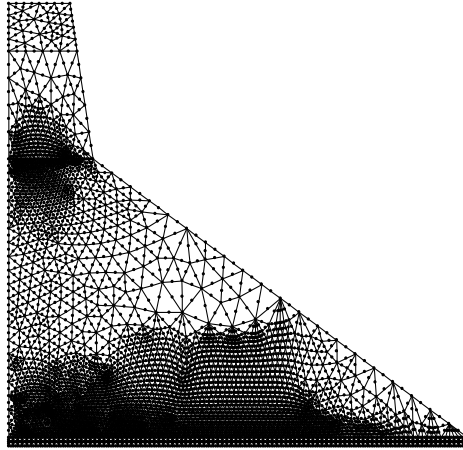


Figure 2: Undeformed mesh of the Koyna dam.

Typical horizontal and vertical displacements at the crest of the dam obtained during the simulations are shown in Fig. 3. These global displacements do not significantly depend on the value of α and are similar to those found in [14] according to LEFM. As expected, horizontal displacements are much higher in modulus than the vertical ones, confirming that modelling Mode Mixity is an important issue for these problems. Moreover, note that the vertical displacements are often negative valued, implying a contact condition at the interface. The evolution of damage along the interface strongly depend on α . Since

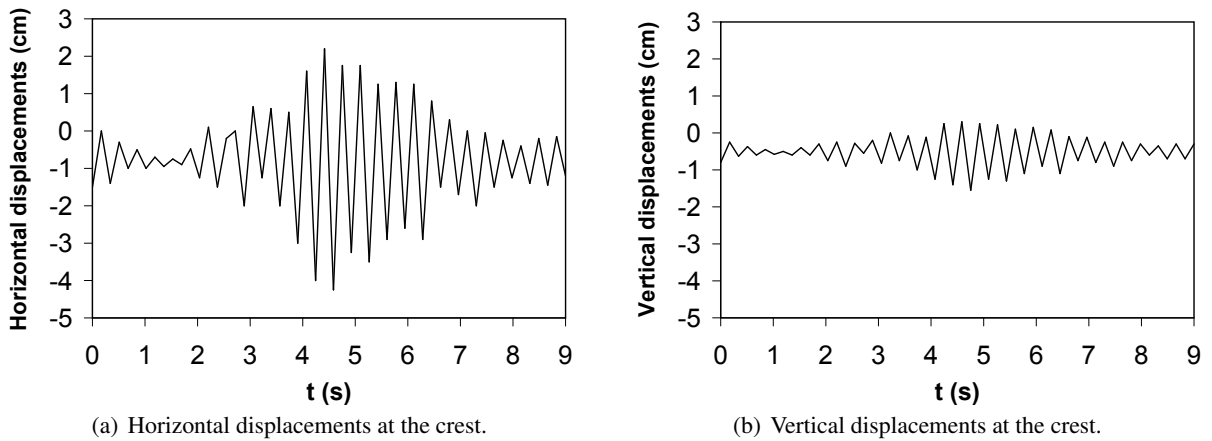


Figure 3: Horizontal and vertical displacements at the crest of the dam vs. time.

the ratio $\Delta g/g_{\max}$ is a quantity lower than unity, the higher the exponent α , the lower is the damage increment. The damage evolution along the rock-concrete interface in the case of $\alpha = 1$ is shown in Fig. 4(a) for different time steps (x denotes the horizontal distance from the upstream of the dam, where crack nucleates). The damage variable D is an increasing function of time and reaches unity for $t = 6.0$ s. Afterwards, no tractions are transmitted along the nucleated real crack, whose final length reaches 1.1 m at $t = 6.3$ s. (see also the deformed mesh in Fig. 5, along with the superimposed contour plot of the equivalent von Mises stresses). On the contrary, when $\alpha = 2$, damage is much lower, being always less

than 0.1 (see Fig. 4(b)).

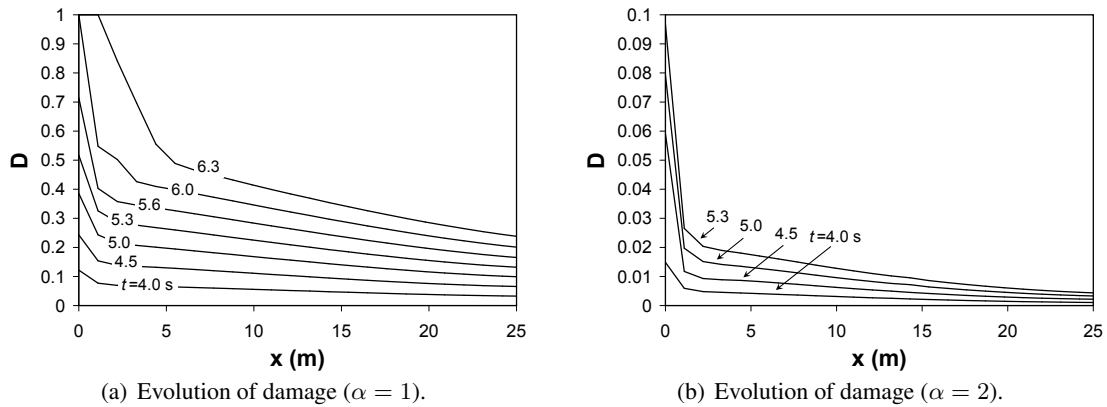


Figure 4: Evolution of damage along the interface vs. time.

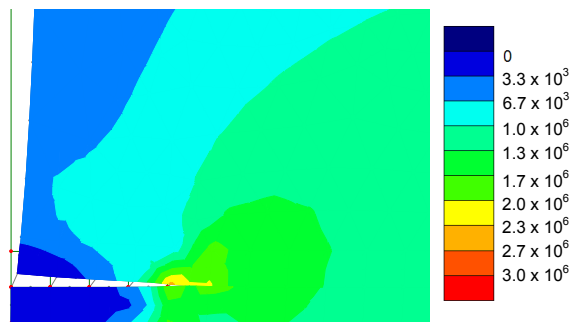


Figure 5: Detail of the deformed mesh near the dam foundation (magnification factor=400) and contour plot of von Mises stresses (Pa).

REFERENCES

- [1] Linsbauer, H.N.: Fracture mechanics models for characterizing crack behaviour of gravity dams, Proc. of the 15th ICOLD, Lausanne (1985) Vol. 2, pp. 279-291.
- [2] Fanelli, M.; Giuseppetti, G.: Advanced dam analysis, Engng. Fract. Mech. (1990) Vol. 35, pp. 525-530.
- [3] Chappell, J.F.; Ingraffea, A.R.: A fracture mechanics investigation of the cracking of Fontana dam, Department of Structural Engineering, Report 81-7, Cornell University, Ithaca, New York (1981).
- [4] Ingraffea, A.R.: Case studies of simulation of fracture in concrete dams, Engng. Fract. Mech. (1990) Vol. 35, pp. 553-564.
- [5] Jirásek, M.; Zimmermann, T.: Analysis of the rotating crack model, J. Engng. Mech. ASCE (1998) Vol. 124, pp. 842-851.
- [6] Lin, Shan-Wern S.; Ingraffea, A.R.: Case studies of cracking of concrete dams-a linear elastic approach, Department of Structural Engineering, Report 88-2, Cornell University, Ithaca, New York (1981).

- [7] Linsbauer, H.N.; Ingraffea, A.R.; Rossmannith, H.P.; Wawrzynek, P.A.: Simulation of cracking in large arch dam: part I, *ASCE J. Struct. Eng.* (1989) Vol. 115, pp. 1599-1615.
- [8] Linsbauer, H.N.; Ingraffea, A.R.; Rossmannith, H.P.; Wawrzynek, P.A.: Simulation of cracking in large arch dam: part II, *ASCE J. Struct. Eng.* (1989) Vol. 115, pp. 1616-1630.
- [9] Linsbauer, H.N.: Application of the methods of fracture mechanics for the analysis of cracking in concrete dams, *Engng. Fract. Mech.* (1990) Vol. 35, pp. 541-551.
- [10] Barpi, F.; Valente S.: Numerical simulation of prenotched gravity dam models, *J. Eng. Mech.* (2000) Vol. 126, pp. 611-629.
- [11] Guanglun, W.; Pekau, O.A.; Chuhan, Z.; Shaomin, W.: Seismic fracture analysis of concrete gravity dams based on nonlinear fracture mechanics, *Eng. Fract. Mech.* (2000) Vol. 65, pp. 67-87.
- [12] Carpinteri, A.; Valente, S.; Ferrara, G.; Imperato, L.: Experimental and numerical fracture modelling of a gravity dam. In: Z.P. Bazant ed., *Fracture Mechanics of Concrete Structures*. Elsevier, The Netherlands (1992) pp. 351-360.
- [13] Chapuis, J.; Rebora, B.; Zimmermann, T.: Numerical approach of crack propagation analysis in gravity dams during earthquakes, *Proc. of the 15th ICOLD, Lausanne* (1985) Vol. 2, pp. 451-473.
- [14] Ayari, M.L.; Saouma, V.E.: A fracture mechanics based seismic analysis of concrete gravity dams using discrete cracks, *Engng. Fract. Mech.* (1990) Vol. 47, pp. 587-598.
- [15] Paggi, M.; Carpinteri, A.; Zavarise, G.: A unified interface constitutive law for the study of fracture and contact problems in heterogeneous materials, In: P. Wriggers, U. Nackenhorst (Eds.), *Analysis and Simulation of Contact Problems, Lecture Notes in Applied and Computational Mechanics* (2006), Springer-Verlag, Berlin, Vol. 27, pp. 297-304.
- [16] Geubelle, P.H., Baylor, J.S.: Impact-induced delamination of composites: a 2D simulation, *Composites Part B: Engineering* (1998) Vol. 29, pp. 589-602.
- [17] Panagiotopoulos, P.D.: *Inequality Problems in Mechanics and Applications*, Birkhäuser Verlag, Basel (1985).
- [18] Roe, K.L., Siegmund, T.: An irreversible cohesive zone model for interface fatigue crack growth simulations, *Engng. Fract. Mech.* (2003) Vol. 70, pp. 209-232.
- [19] Wriggers, P.: *Computational Contact Mechanics*, John Wiley & Sons, Ltd., The Atrium, Southern Gate, Chichester, West Sussex, PO19 8SQ, England (2002).
- [20] Carpinteri, A.; Paggi, M.; Zavarise, G.: The effect of contact on the decohesion of laminated beams with multiple microcracks, *Int. J. Solids Struct.* (2008) Vol. 45, pp. 129-143.
- [21] Zavarise, G.; Boso, D.; Schrefler, B.: A contact formulation for electrical and mechanical resistance, In: *Proceedings of CMIS, III Contact Mechanics International Symposium, Praja de Consolacao, Portugal* (2001) pp. 211218.
- [22] Carpinteri, A.: Scaling laws and renormalization groups for strength and toughness of disordered materials, *Int. J. Solids Struct.* (1994) Vol. 31, pp. 291-302.
- [23] Carpinteri, A.; Ferro, G.: Size effects on tensile fracture properties: a unified explanation based on disorder and fractality of concrete microstructure, *Mater. Struct.* (1994) Vol. 27, pp. 563-571.
- [24] Carpinteri, A.; Chiaia, G.: Multifractal nature of concrete fracture surfaces and size effects on nominal fracture energy, *Mater. Struct.* (1995) Vol. 28, pp. 435-443.
- [25] Corigliano, A.; Mariani, S.; Pandolfi, A.: Numerical analysis of rate-dependent dynamic composite delamination, *Comp. Sci. Tech.* (2006) Vol. 66, pp. 766-775.
- [26] Fishman, Yu. A.: Stability of concrete retaining structures and their interface with rock foundations, *Int. J. Rock Mech. Mining Sci.* (2009) Vol. 46, pp. 957-966.

Corresponding author: marco.paggi@polito.it